Determining the Mechanical Properties of Two-Dimensional 1T-ScX_2 Materials

Huu Tu Nguyen
Faculty of Fundamental Science, Military Academy of Logistics, Hanoi, Vietnam
nguyenhuutu160382@gmail.com

Van Trang Nguyen
Thai Nguyen University of Technology, Thai Nguyen, Vietnam
nvtrang@tnut.edu.vn (corresponding author)

Received: 13 January 2025 | Revised: 12 February 2025 and 02 March 2025 | Accepted: 6 March 2025

 DOI: https://doi.org/10.48084/etasr.10224

ABSTRACT

This study examines the mechanical properties of two-dimensional (2D) materials consisting of scandium and non-metallic elements X (1T-ScX_2, X = O, S, Se, or Te). These parameters , including the elastic modulus, Poisson's ratio, stress, and tensile strain were analyzed using the Atomic Finite Element Method (AFEM) with the Stillinger-Webber potential function. The results revealed that the elastic modulus, E_t of 1T-ScX_2, ranged from 29.39 to 100.69 N/m, Poisson's ratio from 0.142 to 0.215, maximum stress, σ_t, from 3.52 to 11.69 N/m, and tensile strain at break from 0.221% to 0.283%. These findings were then compared to the results of a previous study under the similar conditions. The differences were slight, with errors ranging from -2.03% to 1.21% for E_t, -5.33% to -1.67% for Poisson's ratio, -5.2% to 6.8% for maximum tensile stress, and -8.97% to 1.3% for tensile strain at maximum stress. As the elastic modulus and Poisson's ratio in both studies were quite similar, it can be assumed that 1T-ScX_2 are isometric materials. These findings contribute to the design and application of 2D materials in nanotechnology.

Keywords-Stillinger-Weber; two-dimensional materials; 1T structures; finite elements; tensile tests

I. INTRODUCTION

The discovery of graphene, a 2D nanomaterial consisting of a single atomic layer in 2010 marked the beginning of nanotechnology [1]. Since then, many domestic and international scientists have researched nanometer-sized materials, including their natural occurrence, laboratory synthesis methods, and mechanical, physical, and chemical properties. As a result of these studies, numerous scientific works have been published with many practical applications, such as the use of nanotechnology in electronic devices to manufacture nanometer-sized transistors [2-5], in electronic storage devices [6, 7], in the energy field [8, 9], in the medical field [10], and other areas [11]. Among these materials, the 2D are in the form of a nanometer-sized atomic layer that exist in many different structural systems, such as Pucked structure [5], planar hexagonal graphene [1], low-bucked silicene, BN and AlN [4], 1H and 1T structures [3]. Many findings indicate that 2D materials exhibit special properties, like good electrical and thermal conductivity, outstanding mechanical properties, which are different from those of the materials at the macroscopic scale. For example, some exhibit negative Poisson's ratio [5, 12], or high hardness [13]. Additionally, their bandgap can be tuned by mechanical strain [14-16] or an external electric field without any chemical modification [16-18]. These exceptional properties make 2D materials suitable for various applications, including effect transistors, opto-electronics, spin-electronics, thermo-electrics, sensors, ion batteries, and supercapacitors [19-22].

In this study, the mechanical properties of 2D materials are examined. These compounds consist of the transition metal Sc and non-metallic elements, forming a hexagonal 1T-ScX_2 structure [3], where X is a non-metallic element. This polymorph can occur naturally or be created in the laboratory [3]. Figure 1 illustrates the orthogonal and the axial projection of a basic cell, with the corresponding numbered atoms. Each cell (the rectangle drawn with dashed lines with side size a (Å)) contains nine atoms including three Sc atoms (red) on a plane, each one bonded to six non-metallic atoms X (blue) distributed symmetrically on two planes. The distance between the plane containing Sc and X is denoted as h. Each X atom is bonded to 3 surrounding Sc atoms. The material structure is further characterized by geometric parameters, including the bond length between Sc and X atoms (d_{Sc-X}); the bond angle between X-Sc-X atoms (θ_{ScXX}); and the bond angle between Sc-X-Sc (θ_{XScSc}). a represents the lattice constant.

Conducting experiments to determine the mechanical properties of nanometer size material is often challenging, costly, and unfeasible. As a result, these properties are typically established through experimental simulations or computational methods, such as ab initio calculations, AFEM, Density-Functional Theory (DFT), or Molecular Dynamics (MD).

Through simulations, mechanical properties, such as 2D elastic modulus, E_t (N/m), Poission's ratio, 2D tensile stress, σ_t (N/m), and strain at break, can be calculated. AFEM ensures reliable results, comparable to those obtained from conventional finite element methods [23-26]. This approach utilizes several types of potential functions, including the Stillinger-Weber potential [27], the Tersoff potential [28], and the harmonic potential [29]. For instance, the Stillinger-Webe potential function is applied to 1T-ScX_2 materials to compute the binding energy between atoms. These calculations are then utilized in an algorithm programmed in MATLAB to simulate the membrane tensile test, as clearly presented in Table I [3]. Mechanical properties have been estimated by DFT for silicene [30-31], blue phosphorene, and arsenene [32]. Authors in [3] established Stillinger-Weber potential parameters for 1T-ScX_2 materials and investigated through MD simulations their mechanical properties; however, there is limited research on these properties. In the present study, the mechanical properties of 1T-ScX_2 materials are examined through AFEM using the Stillinger-Weber potential function.

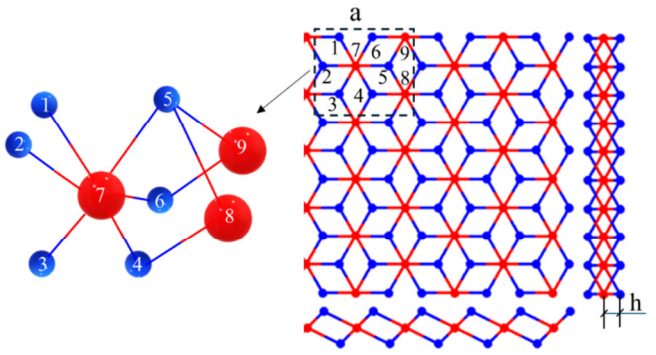

Fig. 1. 1T-ScX_2 material structure, where X represents non-metallic elements (O, S, Se, and Te) belonging to group VIA in the periodic table.

TABLE I. MATERIAL NETWORK PARAMETERS OF 1T-SCX2 MEMBRANE (X=O, S, SE, OR TE) [3].

No.	Materials	Lattice constant, a (Å)	$d_{Sc\text{-}X}$ (Å)	θ_{ScXX} (°)	θ_{XScSc} (°)
1	1T-ScO_2	3.22	2.07	102.115	102.115
2	1T-ScS_2	3.62	2.5	92.771	92.771
3	1T-$ScSe_2$	3.52	2.64	83.621	83.621
4	1T-$ScTe_2$	3.72	2.85	81.481	81.481

II. EXPERIMENTAL SIMULATION BY NUMERICAL METHODS

The AFEM principle is to apply/refers to applying the minimization of potential energy to the atomic interaction potential of the 1T-ScX_2 membrane, as displayed in Figure 1, to determine the stiffness matrix.

For each 1T-ScX_2 membrane, the atomic interaction potential is determined through the parameters of the Stillinger-Weber potential function, including the direct binding energy of two adjacent atoms, Er (eV), and the binding energy of three adjacent atoms, E_θ (eV):

$$E = E_r + E_\theta \quad (1)$$

$$E_r = \sum_{i=1}^{m} V_2 \quad (2)$$

$$E_\theta = \sum_{i=1}^{n} V_3 \quad (3)$$

$$V_2 = A e^{\left[\rho/\left(r_{ij}-r_{\max}\right)\right]}\left(B/r_{ij}^4 - 1\right) \quad (4)$$

$$V_3 = K e^{\left[\rho_{ij}/\left(r_{ij}-r_{\max ij}\right)+\rho_{ik}/\left(r_{ik}-r_{\max ik}\right)\right]}\left(\cos\left(\theta_{ijk}\right)-\cos\left(\theta_0\right)\right)^2 \quad (5)$$

where E is the total atomic bond energy, E_θ is the total angular bond energy of three atoms, E_r is the total linear bond energy between two atoms of the membrane, V_2 (eV) is the linear bond energy of two adjacent atoms, V_3 (eV) is the angular bond energy of three adjacent atoms, m, n are the numbers of linear and angular bonds, respectively, A (eV), and K (eV) are the material coefficients, ρ (Å), B (Å^4), ρ_{ij} (Å), and ρ_{ik} (Å), θ_o (degrees) are the geometric parameters of the material, r_{ij} (Å) and r_{ik} (Å) are the bond lengths between three i, j, and k, atoms, θ_{ijk} (degrees) is the the bond angle between three i, j, k atoms with i being the middle atom, as depicted in Figure 2.

These parameters are summarized in Tables II and III [3].

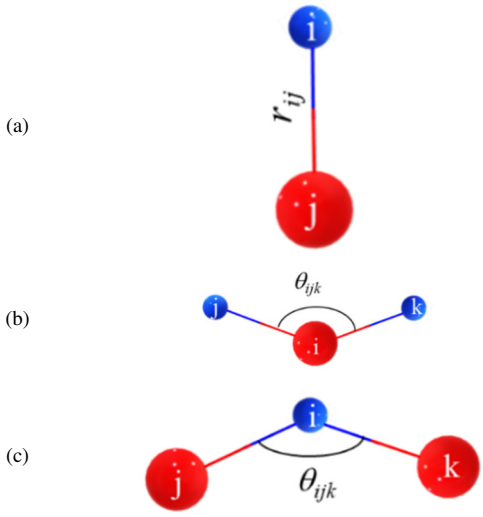

Fig. 2. AFEM when using Stillinger-Weber potential function: (a) straight bond between two atoms and (b),(c) angular bond between 3 atoms.

For each 1T-ScX2 membrane, the total number of atoms is N. X_i and u_i are the initial coordinates and displacement of the i-th atom, respectively. After deformation, the new coordinates of the atom are given by:

$$x_i = X_i + u_i$$

TABLE II. STILLINGER-WEBER POTENTIAL FUNCTION PARAMETERS FOR THE STRAIGHT BOND OF MATERIAL 1T-SCX$_2$ V_2 [3]

No.	Materials	Bond	A (eV)	ρ(Å)	B (Å^4)	r_{min} (Å)	r_{max} (Å)
1	1T-ScO_2	Sc-O	10.187	1.493	9.180	0.0	2.949
2	1T-ScS_2	Sc-S	3.516	1.443	19.531	0.0	3.450
3	1T-$ScSe_2$	Sc-Se	3.884	1.173	24.288	0.0	3.520
4	1T-$ScTe_2$	Sc-Te	4.269	1.183	32.988	0.0	3.768

TABLE III. STILLINGER-WEBER POTENTIAL FUNCTION PARAMETERS FOR ANGLE BOND OF THE 1T-SCX$_2$ V_3 [3]

No.	Materials	Angular bond	K (eV)	θ_0 (°)	ρ_1 (Å)	ρ_2 (Å)	r_{min1} (Å)	r_{max12} (Å)	r_{min13} (Å)	r_{max13} (Å)	r_{min23} (Å)	r_{max23} (Å)
1	1T-ScO_2	θ_{ScOO}	50.913	102.115	1.493	1.493	0.0	2.949	0.0	2.949	0.0	4.399
		θ_{OScSc}	50.913	102.115	1.493	1.493	0.0	2.949	0.0	2.949	0.0	4.399
2	1T-ScS_2	θ_{ScSS}	16.674	92.771	1.443	1.443	0.0	3.450	0.0	3.450	0.0	4.945
		θ_{SScSc}	16.674	92.771	1.443	1.443	0.0	3.450	0.0	3.450	0.0	4.945
3	1T-$ScSe_2$	θ_{ScSeSe}	17.479	83.621	1.173	1.173	0.0	3.520	0.0	3.520	0.0	4.808
		θ_{SeScSc}	17.479	83.621	1.173	1.173	0.0	3.520	0.0	3.520	0.0	4.808
4	1T-$ScTe_2$	θ_{ScTeTe}	16.139	81.481	1.183	1.183	0.0	3.768	0.0	3.768	0.0	5.082
		θ_{TeScSc}	16.139	81.481	1.183	1.183	0.0	3.768	0.0	3.768	0.0	5.082

The atomic interaction potential of the entire membrane calculated by (1) is a function that depends only on the coordinates of each atom:

$$E = E\left(\mathrm{x}_1, \mathrm{x}_2, ..., \mathrm{x}_N\right) \quad (6)$$

On the other hand, when the membrane is subjected to an external force f_i on the i-th atom (considered as nodes), the atoms have displacements u_i correspondingly, the potential energy of the applied external force is calculated by:

$$E_{ext} = \sum_{i=1}^{N} f_i u_i \quad (7)$$

So, the total potential energy of the membrane is:

$$\Pi = E - E_{ext} \quad (8)$$

The membrane is in equilibrium when the Π reaches its minimum value according to the principle of minimum potential energy. Therefore, the first derivative of the total potential energy will be zero:

$$\frac{\partial \Pi}{\partial u_i} = 0, \; i = 1, ..., N \quad (9)$$

Equation (9) is expressed in the finite element form, using the Newton–Raphson iteration method [25-27]:

$$K^{(k)} u^{(k)} = F^{(k)} \quad (10)$$

$$K_{ij}^{k} = \frac{\partial^2 \Pi^{(k)}}{\partial u_i \partial u_j}; F_i^{(k)} = -\frac{\partial \Pi^{(k)}}{\partial u_i} = f_i - \frac{\partial E^{(k)}}{\partial u_i}; \quad (11)$$

where $K^{(k)}$ is the global stiffness matrix, $u^{(k)}$ is the nodal displacement vector, and $F^{(k)}$ is the nodal force vector. Equations (10) and (11) are the basic equations of the finite element method. When each atom is considered as a node, its displacement corresponds to the displacement of that node. Due to the structure of the orthogonal hexagonal membrane, as illustrated in Figure 1, two types of elements are formed:

- 3-node elements (Valence): These present molecules on the boundary of the membrane, where each element consists of three bonded atoms.
- 4-node elements (Improper): These elements are detected inside the membrane, each bonded by four atoms, as depicted in Figure 3.

Since each atom can move in three directions, (11) is used to calculate the stiffness matrix of each element with dimensions $\left[K_{val}\right]_{9x9}^{(e)}$;$\left[K_{\mathrm{Im}p}\right]_{12x12}^{(e)}$, corresponding to 3-node and 4-node elements. From this matrix, the global stiffness matrix $\left[K\right]_{3Nx3N}^{(k)}$ is computed, which is the composite matrix of the element stiffness matrices over the entire membrane. The displacement vectors and force vectors have dimensions corresponding to the global stiffness matrix.

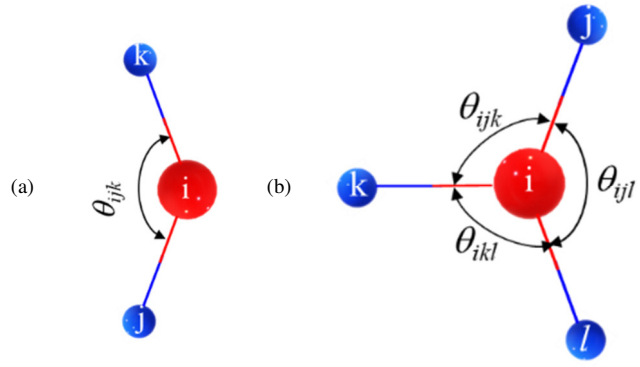

Fig. 3. Element model using the AFEM: (a) the Valence element formed by three adjacent atoms, (b) the Improver element formed by four adjacent atoms.

Equation (10) is solved using the Newton–Raphson iteration method with displacement boundary conditions i.e., atoms on the tensile boundary, as shown in Figure 4(a), have displacement equal to $u(0)$, and atoms on the retaining boundary, as portrayed in Figure 4(b), have no displacement in the tensile direction.

III. RESULTS AND DISCUSSION

The experimental model of the whole membrane tensile test is presented in Figure 4 through the displacement method.

In the simulation, a rectangular membrane with equal side dimensions (the rectangle is considered to be a square) is subjected to tensile loading. Each membrane consists of 4,200 atoms. Each stretching step causes the atoms on the stretching edge to move with an increment of $\delta\varepsilon = 0.001$. This process is repeated until a bond breaks leading to membrane destruction. The position of atoms in the next steps is determined by:

$$x_{(k+1)} = x_{(k)} + u_{(k)} \quad (12)$$

The iterative process continues until the membrane's failure. The data of the entire simulation across all steps are synthesized to obtain the key mechanical parameters.

The tensile findings of 1T-ScX_2 materials are analyzed through stress-strain relationship graphs. The 2D elastic modulus is determined by linearizing this curve within the range of 0 to 0.1. The Poisson's ratio is calculated based on the ratio of transverse strain and axial strain, expressed as:

$$\nu = -\varepsilon_y/\varepsilon_x \quad (13)$$

The stress-strain relationship when stretching the intact membranes of the four materials is illustrated in Figure 5. The maximum values of those parameters are summarized in Table IV [3].

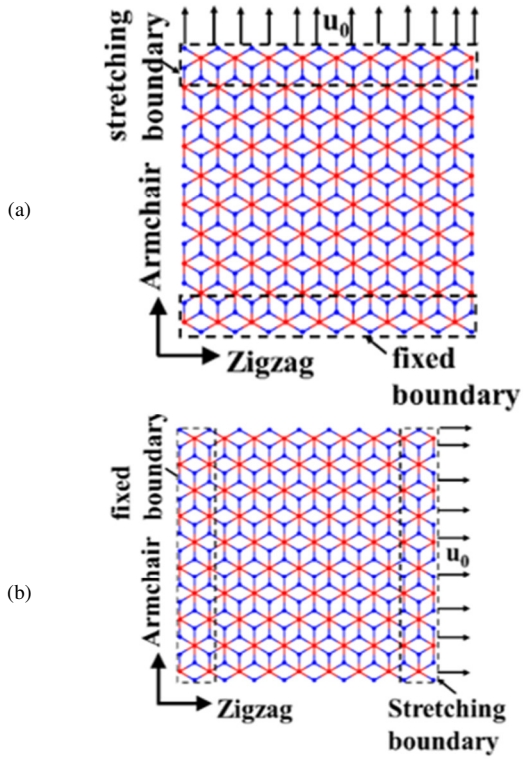

Fig. 4. Membrane stretching with displacement boundary conditions: (a) in the armchair direction, (b) in the zigzag direction.

TABLE IV. MECHANICAL PARAMETERS OF FOUR 1T-SCX_2 MATERIALS AND COMPARISON WITH [3] RESULTS

No.	Materials	Stretching directions	Elastic modulus, E_t (N/m)	Poisson's ratio	Maximum stress, σ_t (N/m)	Tensile strain	Evaluations
1	1T-ScO2	AC	99.85	0.143	11.69	0.221	present results
			100.9	0.15	11.7	0.22	by MD at 10 K [3]
			-1.04	-4.67	-0.09	0	error (%) with [3]
		ZZ	100.69	0.142	10.99	0.235	present results
			100.4	0.15	11.3	0.25	by MD at 10 K [3]
			0.29	-5.33	-274	-6	error (%) with [3]
2	1T-ScS2	AC	29.39	0.167	4.05	0.233	present results
			30	0.17	3.8	0.23	by MD at 10 K [3]
			-2.03	-1.76	6.58	1.3	error (%) with [3]
		ZZ	29.67	0.166	3.52	0.25	present results
			29.9	0.17	3.6	0.27	by MD at 10 K [3]
			-0.77	-2.35	-2.22	-7.41	error (%) with [3]
3	1T-ScSe2	AC	36.02	0.194	5.18	0.249	present results
			36.4	0.2	5.3	0.25	by MD at 10 K [3]
			-1.04	-3	-2.26	-0.4	error (%) with [3]
		ZZ	36.41	0.192	4.82	0.264	present results
			36.3	0.2	5	0.29	by MD at 10 K [3]
			0.3	-4	-3.6	-8.97	error (%) with [3]
4	1T-ScTe2	AC	31.29	0.215	5.06	0.264	present results
			31.4	0.22	5.2	0.27	by MD at 10 K [3]
			-0.35	-2.27	-2.69	-2.22	error (%) with [3]
		ZZ	31.68	0.213	4.74	0.283	present results
			31.3	0.22	5	0.31	by MD at 10 K [3]
			1.21	-3.18	-5.2	-8.71	error (%) with [3]

For 2D materials, the 2D elastic modulus, E_t (N/m), and the 2D stress, σ_t (N/m), depend on the membrane's thickness, t. When t is in nanometer, E_t values are extremely high, which can be much larger than the steel hardness. For example, if graphene's thickness is $t \approx 3.4$ Å, $E_t = 358$ N/m in the zigzag direction, and $E_t = 340$ N/m in the armchair direction. At that

time, the elastic modulus of graphene is E ≈ 1.05×10^{12} N/m^2 and E ≈ 1.03×10^{12} N/m^2, respectively [13]. In this study, when stretching the original membrane of four 1T-ScX_2 materials, E_t ranges from 29.39 to 100.69 N/m, Poisson's ratio ranges from 0.142 to 0.215, σ_t ranges from 3.52 to 11.69 N/m, while the strain at break ranges from 0.221% to 0.283%. These results were compared with the research findings of [3] under the same experimental simulation conditions. The comparison revealed minor discrepancies. Specifically, the error in E_t ranged from -2.03% to 1.21%, the error in Poisson's ratio ranged from -5.33% to -1.67%, the error in maximum tensile stress ranged from -5.2% to 6.8%, and the error in strain at maximum stress ranged from -8.97% to 1.3%.

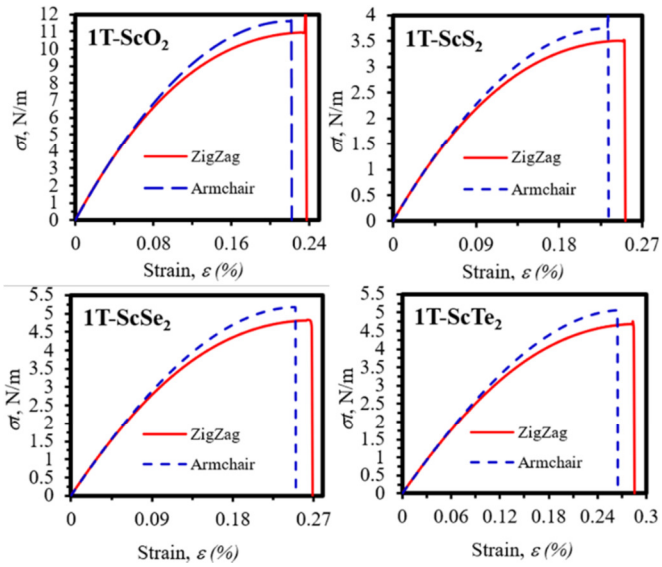

Fig. 5. Stress and strain relationship when strentching 1T-ScX_2 membrane.

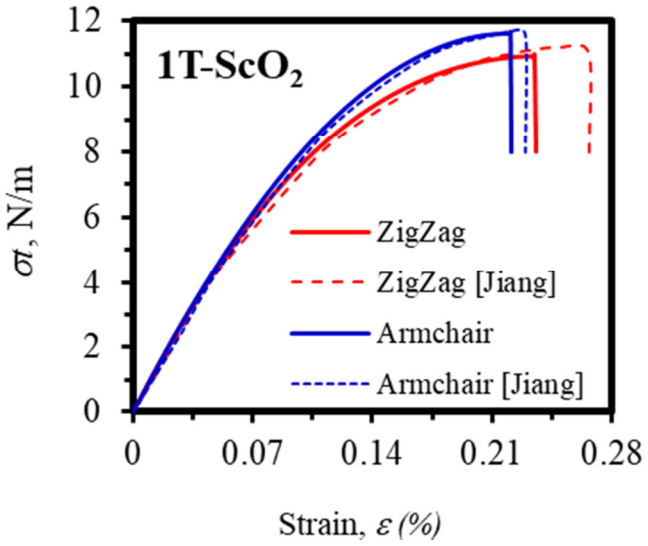

Fig. 6. Stress-strain relationship when stretching 1T-ScO_2 membrane.

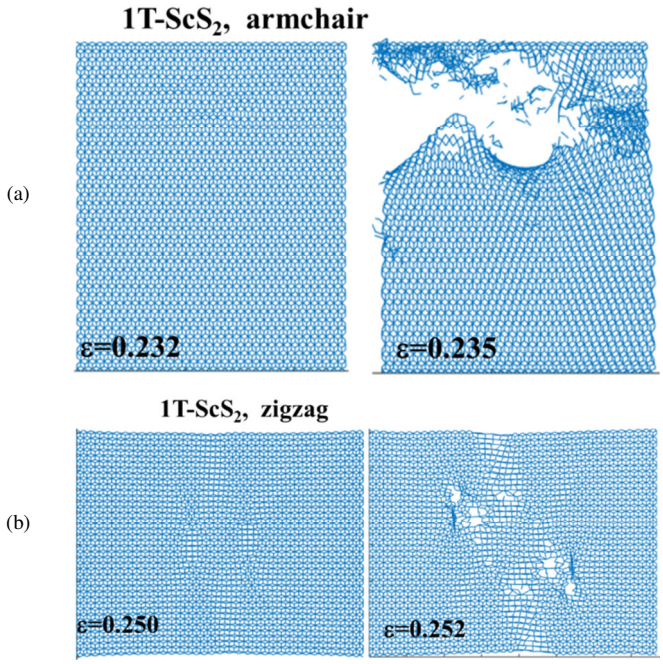

Fig. 7. Tensile failure of 1T-ScS_2 membranes: (a) armchair tensile strain, (b) zigzag tensile strain.

Figure 6 displays the relationship between stress and strain when stretching 1T-ScO_2 membrane. The solid line is the result of this study, while the dashed line is the result of [3]. It is evident that these lines are almost identical. However, when using MD [3] to pull, the membrane exhibits a maximum strain before being destroyed. The destruction of the membrane occurs when the bonds between adjacent atoms are broken according to the conditions set in the calculation program. Figure 7 depicts the destruction of the 1T-ScS_2 membrane when stretching in the armchair direction, with $\varepsilon = 0.235\%$, and when stretching in the zigzag direction, with $\varepsilon = 0.252\%$, many bonds were broken, and the membrane was destroyed.

IV. CONCLUSIONS

The current research investigated the mechanical properties of four orthogonally symmetric two-dimensional (2D) materials (1T-ScX_2) using the Atomic Finite Element Method (AFEM) with the Stillinger-Weber potential function. The results were compared to previous research under the same conditions [3]. The results showed that E_t ranged from 29.39 to 100.69 N/m, Poisson's ratio from 0.142 to 0.215, maximum stress, σ_t, from 3.52 to 11.69 N/m, and tensile strain from 0.221% to 0.283%. The comparison revealed errors ranging from -2.03% to 1.21% for E_t, -5.33% to -1.67% for Poisson's ratio, -5.2% to 6.8% for maximum tensile stress, and -8.97% to 1.3% for tensile strain at maximum stress. These close values indicate that these materials exhibit isotropic mechanical behavior.

ACKNOWLEDGMENT

This work has been supported by Thai Nguyen University of Technology.

REFERENCES

[1] A. K. Geim, "Graphene: Status and Prospects," *Science*, vol. 324, no. 5934, pp. 1530–1534, Jun. 2009, https://doi.org/10.1126/science.1158877.

[2] F. Hao and X. Chen, "First-principles study of the defected phosphorene under tensile strain," *Journal of Applied Physics*, vol. 120, no. 16, Oct. 2016, Art. no. 165104, https://doi.org/10.1063/1.4966167.

[3] J. W. Jiang, *Handbook of Stillinger-Weber Potential Parameters for Two-Dimensional Atomic Crystals,* 2017. Available: https://www.intechopen.com/books/6638.

[4] H.-T. Nguyen, M.-Q. Le, and V.-T. Nguyen, "Mode-I stress intensity factors of silicene, AlN, and SiC hexagonal sheets," *Materials Research Express*, vol. 5, no. 6, Mar. 2018, Art. no. 065025, https://doi.org/10.1088/2053-1591/aac807.

[5] Minh Q. L., Hữu T. N., Kim L. Đ. T., and Văn T. N., "Tensile simulation of two-dimensional polyatomic materials with pleated structures," *Journal of Transport Science*, vol. 73, no. 5, pp. 514–526, 2022, https://doi.org/10.47869/tcsj.73.5.6.

[6] L. Li *et al.*, "Black phosphorus field-effect transistors," *Nature Nanotechnology*, vol. 9, no. 5, pp. 372–377, May 2014, https://doi.org/10.1038/nnano.2014.35.

[7] D. Staros, B. Rubenstein, and P. Ganesh, "A first-principles study of bilayer 1T'-WTe2/CrI3: a candidate topological spin filter," *npj Spintronics*, vol. 2, no. 1, Apr. 2024, Art. no. 4, https://doi.org/10.1038/s44306-023-00007-y.

[8] M. B. Tahir, N. Fatima, U. Fatima, and M. Sagir, "A review on the 2D black phosphorus materials for energy applications," *Inorganic Chemistry Communications*, vol. 124, Feb. 2021, Art. no. 108242, https://doi.org/10.1016/j.inoche.2020.108242.

[9] S. A. Ogunkunle *et al.*, "Defect engineering of 1T′ MX2 (M = Mo, W and X = S, Se) transition metal dichalcogenide-based electrocatalyst for alkaline hydrogen evolution reaction," *Journal of Physics: Condensed Matter*, vol. 36, no. 14, Jan. 2024, Art. no. 145002, https://doi.org/10.1088/1361-648X/ad19a4.

[10] M. Luo, T. Fan, Y. Zhou, H. Zhang, and L. Mei, "2D Black Phosphorus–Based Biomedical Applications," *Advanced Functional Materials*, vol. 29, no. 13, 2019, Art. no. 1808306, https://doi.org/10.1002/adfm.201808306.

[11] S. Santra, M. S. Ali, S. Karmakar, and D. Chattopadhyay, "Molybdenum disulfide: A nanomaterial that is paving the way toward a sustainable future," *Materials Today Sustainability*, vol. 25, Mar. 2024, Art. no. 100659, https://doi.org/10.1016/j.mtsust.2023.100659.

[12] L. Yu, Q. Yan, and A. Ruzsinszky, "Negative Poisson's ratio in 1T-type crystalline two-dimensional transition metal dichalcogenides," *Nature Communications*, vol. 8, no. 1, May 2017, Art. no. 15224, https://doi.org/10.1038/ncomms15224.

[13] M.-Q. Le and R. C. Batra, "Mode-I stress intensity factor in single layer graphene sheets," *Computational Materials Science*, vol. 118, pp. 251–258, Jun. 2016, https://doi.org/10.1016/j.commatsci.2016.03.027.

[14] D. Singh, S. K. Gupta, I. Lukačević, and Y. Sonvane, "Indiene 2D monolayer: a new nanoelectronic material," *RSC Advances*, vol. 6, no. 10, pp. 8006–8014, Jan. 2016, https://doi.org/10.1039/C5RA25773E.

[15] Z. Zhu and D. Tománek, "Semiconducting Layered Blue Phosphorus: A Computational Study," *Physical Review Letters*, vol. 112, no. 17, May 2014, Art. no. 176802, https://doi.org/10.1103/PhysRevLett.112.176802.

[16] J.-A. Yan, S.-P. Gao, R. Stein, and G. Coard, "Tuning the electronic structure of silicene and germanene by biaxial strain and electric field," *Physical Review B*, vol. 91, no. 24, Jun. 2015, Art. no. 245403, https://doi.org/10.1103/PhysRevB.91.245403.

[17] A. Molle, J. Goldberger, M. Houssa, Y. Xu, S.-C. Zhang, and D. Akinwande, "Buckled two-dimensional Xene sheets," *Nature Materials*, vol. 16, no. 2, pp. 163–169, Feb. 2017, https://doi.org/10.1038/nmat4802.

[18] Z. Ni *et al.*, "Tunable Bandgap in Silicene and Germanene," *Nano Letters*, vol. 12, no. 1, pp. 113–118, Jan. 2012, https://doi.org/10.1021/nl203065e.

[19] P. Vishnoi, K. Pramoda, and C. N. R. Rao, "2D Elemental Nanomaterials Beyond Graphene," *ChemNanoMat*, vol. 5, no. 9, pp. 1062–1091, 2019, https://doi.org/10.1002/cnma.201900176.

[20] D. Geng and H. Y. Yang, "Recent Advances in Growth of Novel 2D Materials: Beyond Graphene and Transition Metal Dichalcogenides," *Advanced Materials*, vol. 30, no. 45, 2018, Art. no. 1800865, https://doi.org/10.1002/adma.201800865.

[21] F. Wang *et al.*, "2D library beyond graphene and transition metal dichalcogenides: a focus on photodetection," *Chemical Society Reviews*, vol. 47, no. 16, pp. 6296–6341, Aug. 2018, https://doi.org/10.1039/C8CS00255J.

[22] B. Liu and K. Zhou, "Recent progress on graphene-analogous 2D nanomaterials: Properties, modeling and applications," *Progress in Materials Science*, vol. 100, pp. 99–169, Feb. 2019, https://doi.org/10.1016/j.pmatsci.2018.09.004.

[23] A. Ahmed and A. M. I. Said, "The Effect of Expansion Ratio, Opening Size, and Prestress Strand on the Flexural Behavior of Steel Beams with Expanded Web using FEA," *Engineering, Technology & Applied Science Research*, vol. 14, no. 3, pp. 14257–14265, Jun. 2024, https://doi.org/10.48084/etasr.7254.

[24] B. Liu, Y. Huang, H. Jiang, S. Qu, and K. C. Hwang, "The atomic-scale finite element method," *Computer Methods in Applied Mechanics and Engineering*, vol. 193, no. 17, pp. 1849–1864, May 2004, https://doi.org/10.1016/j.cma.2003.12.037.

[25] Y. Wang *et al.*, "Atomistic finite elements applicable to solid polymers," *Computational Materials Science*, vol. 36, no. 3, pp. 292–302, Jun. 2006, https://doi.org/10.1016/j.commatsci.2005.03.016.

[26] J. Wackerfuß, "Molecular mechanics in the context of the finite element method," *International Journal for Numerical Methods in Engineering*, vol. 77, no. 7, pp. 969–997, 2009, https://doi.org/10.1002/nme.2442.

[27] F. H. Stillinger and T. A. Weber, "Computer simulation of local order in condensed phases of silicon," *Physical Review B*, vol. 31, no. 8, pp. 5262–5271, Apr. 1985, https://doi.org/10.1103/PhysRevB.31.5262.

[28] J. Tersoff, "Modeling solid-state chemistry: Interatomic potentials for multicomponent systems," *Physical Review B*, vol. 39, no. 8, pp. 5566–5568, Mar. 1989, https://doi.org/10.1103/PhysRevB.39.5566.

[29] D.-T. Nguyen, M.-Q. Le, T.-L. Bui, and H.-L. Bui, "Atomistic simulation of free transverse vibration of graphene, hexagonal SiC, and BN nanosheets," *Acta Mechanica Sinica*, vol. 33, no. 1, pp. 132–147, Feb. 2017, https://doi.org/10.1007/s10409-016-0613-z.

[30] H. Zhao, "Strain and chirality effects on the mechanical and electronic properties of silicene and silicane under uniaxial tension," *Physics Letters A*, vol. 376, no. 46, pp. 3546–3550, Oct. 2012, https://doi.org/10.1016/j.physleta.2012.10.024.

[31] B. Mortazavi, O. Rahaman, M. Makaremi, A. Dianat, G. Cuniberti, and T. Rabczuk, "First-principles investigation of mechanical properties of silicene, germanene and stanene," *Physica E: Low-dimensional Systems and Nanostructures*, vol. 87, pp. 228–232, Mar. 2017, https://doi.org/10.1016/j.physe.2016.10.047.

[32] G. Liu, Z. Gao, and J. Zhou, "Strain effects on the mechanical properties of Group-V monolayers with buckled honeycomb structures," *Physica E: Low-dimensional Systems and Nanostructures*, vol. 112, pp. 59–65, Aug. 2019, https://doi.org/10.1016/j.physe.2019.04.002.